Bulg. J. Phys. **35** (2008) 33–52

Two-Resonator Method for Characterization of Dielectric Substrate Anisotropy

V.N. Levcheva, **B.N. Hadjistamov**, **P.I. Dankov**

Faculty of Physics, University of Sofia "St. Kliment Ohridski",
5 J. Bourchier Blvd., 1164 Sofia, Bulgaria

Received *23 May 2008*

Abstract. A two-resonator method, based on TE_{011}-mode and TM_{010}-mode resonance cavities with a disk sample has been developed for measurement of the longitudinal and transversal dielectric constants and dielectric loss tangent of dielectric substrates (dielectric anisotropy), used in modern electronics. The theoretical background of the method is presented: the analytical expressions of the dispersion equations for the considered modes in both cavities and expressions of the energy balance for computation of the permittivity and the dielectric loss tangent of the unknown sample in two directions. The sensitivity and the measurement errors are discussed. Practical examples are given for illustration of the dielectric anisotropy characterization of modern reinforced substrates with built-in woven glass cloth and filling plastics or powders.

PACS number: 77.22. – d

1 Introduction

The full characterization of dielectric properties of materials is very important for the modern RF design. This obvious fact corresponds to the necessity of fast and accurate simulations of the S-parameters of the designed devices by powerful fast-developing structure and schematic simulators. Usually the designers rely upon the catalogue data for the relative dielectric constant ε_r and dielectric loss tangent $\tan\delta_\varepsilon$ (dissipation factor), obtained by the IPC TM-650 2.5.5.5 stripline-resonator test method [1] giving parameters $\varepsilon'_\perp$ and $\tan\delta_{\varepsilon\perp}$ (near-to-transversal values, *i.e.* normal to the substrate surface). Unfortunately, they might be insufficient in many design cases. It is known that designers "tune" the dielectric constant about the catalogue values in order to fit the simulated and measured dependences for the designed device. The problem appears, because the modern substrates have dielectric anisotropy, *i.e.* different values of the longitudinal and transversal dielectric constant ($\varepsilon'_{||} \neq \varepsilon'_\perp$) and dielectric

loss tangent ($\tan\delta_{\varepsilon||} \neq \tan\delta_{\varepsilon\perp}$). In several of our previous papers [2–4] we have established that the most of the commercial reinforced laminates (with layers of woven glass, ceramic powders, organic filling, *etc.*) have a noticeable dielectric anisotropy (*e.g.* up to 15–25% for dielectric constant anisotropy $\Delta A_\varepsilon = 2|\varepsilon'_{||} - \varepsilon'_\perp|/\varepsilon'_{||} + \varepsilon'_\perp)$ and up to 50–80% for dielectric loss tangent anisotropy $\Delta A_{\tan\delta\varepsilon} = 2|\tan\delta_{\varepsilon||} - \tan\delta_{\varepsilon\perp}|/(\tan\delta_{\varepsilon||} + \tan\delta_{\varepsilon\perp})$. In fact, suitable information about the dielectric anisotropy of substrates and materials can not be found in the producers data catalogues. As a rule, they include rather common parameter values, which specify a kind of a manufactured artificial material, but do not specify the variations from the production lots, from the sample thickness, *etc.* Neglecting the anisotropy may decrease the RF design accuracy for many microwave components and devices – coplanar waveguides and feeds, radiating patches, filters, dividers, stubs, matching components, *etc.* [5–6]. An additional problem appears for some artificial substrates and films with a measurable local inhomogeneity of the dielectric constant along a given direction [7].

We have proposed in [3,4] a very convenient and relatively universal two-resonator method for accurate characterization of the dielectric anisotropy ΔA_ε and $\Delta A_{\tan\delta\varepsilon}$ of planar multi-layer samples. In this paper we summarize the theoretical background of the two-resonator method in the simplest case – characterization of single-layer anisotropic substrates. Two different cylindrical resonators are used for this purpose, which support two suitable azimuthally symmetrical modes – TE_{011} mode for the determination of $\varepsilon'_{||}$, $\tan\delta_{\varepsilon||}$ and TM_{010} mode – for $\varepsilon'_\perp$, $\tan\delta_{\varepsilon\perp}$ (see Figure 1a, b).

The idea to use TE_{011}- and TM_{010}-mode resonators for complex dielectric constant measurements of dielectric substrates is not new. Several resonance methods for low-loss dielectric properties characterization have been presented in literature (for example, see a useful comparison in [8]). Most of them are accepted

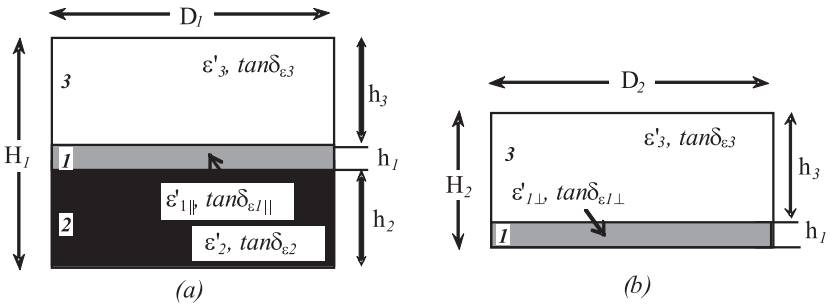

Figure 1. Two types of measuring cavities: a) TE_{011}-mode cavity (**R1**); b) TM_{010}-mode cavity ($R2$) ($h_2 = 0$); both with single-layer sample 1; 2, 3 – foam (or air) filled parts (not to scale).

in metrology institutions like NIST [9] and NPL [10] as reference methods, but as a rule for isotropic materials. However, there is no universal solution for the dielectric anisotropy measurements. Usually, the parameters $\varepsilon'_{||}$ and $\tan\delta_{\varepsilon||}$ can be separately measured using TE-mode resonance cavities (classical Courtney's method [11], Kent's evanescent-mode tester [12], NIST mode-filtered resonator [13], split-cylinder resonator [14], *etc.*). The parameters $\varepsilon'_{\perp}$ and $\tan\delta_{\varepsilon\perp}$ can be estimated using TM-mode resonance cavities [15], low-frequency reentrant cavities [16], *etc.* In fact, only a few publications have been directly dedicated to dielectric-anisotropy measurements. Whispering-gallery modes in single dielectric resonator could be used for anisotropy measurements of ultra and extremely low-loss materials [17,18]. A split-cavity method for the dielectric-constant anisotropy determination through a long cylindrical cavity with TE_{111} and TM_{nm0} modes is described in [19] and data for some reinforced materials are presented. Characterization of the anisotropy of prismatic samples with big dielectric constants is considered in [20].

The goal of our investigations is to present a workable, universal and accurate resonance method based on simple laboratory equipment for measurements of the dielectric anisotropy of *one* dielectric sample using *two* cavity resonators. Therefore, the variations of the properties from sample to sample could be avoided. The proposed method allows easy estimation of the dielectric parameters of anisotropic substrates with different thickness. The collected pairs of measured values ($\varepsilon'_{||}$ and $\tan\delta_{\varepsilon||}$; $\varepsilon'_{\perp}$ and $\tan\delta_{\varepsilon\perp}$) for concrete artificial substrates can be used in microwave simulators for design purposes and for quantitative characterization of the technological processes for new materials.

2 Two Resonance Cylindrical Cavities with Single-Layer Samples

The necessary analytical expressions for determination of the dielectric constant and dielectric loss tangent of single-layer anisotropic substrates by the two-resonator method are presented below.

2.1 Dispersion Equations for Determination of the Dielectric-Constant Anisotropy in Single-Layer Substrates

A three-part resonance cavity is represented in Figure 1, where the parameters of the separate layers are denoted. The dielectric substrate sample 1 is placed between two dielectric supporting parts 2 and 3, usually foam (or air) filled. Two different resonance cavities are proposed for determination of the dielectric constants in two directions – along the resonator axis and perpendicularly to it. When the sample (layers 1) is placed in the resonator's half-height $H_1/2$, the excited TE_{011} mode in the resonance cavity (**R1**) can be used for determination of the longitudinal dielectric constant $\varepsilon'_{||}$ of the sample. This is because the electric field is orientated along its surfaces and it has maximum at $H_1/2$ –

Figure 1a. It is better to choose a resonator with equal diameter and height $D_1 \cong H_1(= h_1 + h_2 + h_3)$ in order to separate the TE_{011} mode from the other low- and high-order modes. The other type of resonator (**R2**) is designed to support the TM_{010} mode, which electric field is orientated normally to the sample surface (for determination of $\varepsilon'_{\perp}$ – Figure 1b). The sample is placed on the resonator floor ($h_2 = 0$). The resonator R2 should have small enough height $H_2 \leq D_2/2$ or even $\cong D_2/3$ to move the higher-order modes (such as TE modes) away from the TM_{010} mode resonance curve.

The exact dispersion equations for the TE and TM modes in the resonance cavities considering lossless samples ($\tan\delta_{\varepsilon 1,2,3} = 0$) can be described as follows:

1) *Dispersion equation for* TE_{nmp} *modes* ($n = 0, 1, 2\ldots;\ m = 1, 2, 3\ldots;\ p = 1, 2, 3\ldots$) – Figure 1a:

$$\left(\frac{\tan\beta_1 h_1}{\beta_1} + \frac{\tan\beta_3 h_3}{\beta_3}\right) + \frac{\tan\beta_2 h_2}{\beta_2}\ \left(1 - \frac{\beta_1}{\beta_3}\tan\beta_1 h_1.\ \tan\beta_3 h_3\right) = 0 \tag{1}$$

2) *Dispersion equation for* TM_{nmp} *modes* ($n = 0, 1, 2\ldots;\ m = 1, 2, 3\ldots;\ p = 0, 1, 2, \ldots$) – Figure 1b ($h_2 \equiv 0$):

$$\left(\frac{\beta_1}{\varepsilon_1}\tan\beta_1 h_1 + \frac{\beta_3}{\varepsilon_3}\tan\beta_3 h_3\right) = 0. \tag{2}$$

These dispersion equations were obtained using known analytical procedures, satisfying the boundary conditions at the perfect cavity walls and between the lossless layers [21].

The propagation constants β_i ($i = 1, 2, 3$) in equations (1) and (2) are expressed for the different layers as $\beta_i^2 = (2\pi/\lambda_0)^2\varepsilon_i - (\chi_{nm})^2_{\mathrm{TE,TM}}/R^2$, where $\lambda_0 = c/f_{res}$; $R = R_{1,2} = D_{1,2}/2$, (f_{res} is the resonance frequency of the given mode excited in the cavity, λ_0 is the free-space wavelength). For the considered resonators $(\chi_{0m})_{TE} = \nu'_{0m} = 3.8317$, 7.1556, 10.1735…– for TE_{011}, TE_{021}, TE_{031} modes and $(\chi_{0m})_{TM} = \nu_{0m} = 2.4048$, 5.5201, 8.6537…– for TM_{010}, TM_{020}, TM_{030} modes ($\nu_0;\ \nu'_0$ are the zeroes of a first-kind Bessel function $J_0(x)$ and its derivative $J'_0(x)$ according to the argument). The dielectric constants ε_i in all layers ($i = 1, 2, 3$) represent either the real part of the longitudinal values $\varepsilon'_{||i}$ (for TE_{0mp} modes) or the real part of the transversal values $\varepsilon'_{\perp i}$ (for TM_{0m0} modes). It is important to note that the type of the tangent functions in the expressions (1) and (2) depend on the β_i^2 values. If $\beta_i^2 > 0$, these functions are ordinary oscillating tangents $\tan(\beta_i h_i)$, but if $\beta_i^2 < 0$ (*i.e.* $\beta_i \to j\alpha_i$) they convert into hyperbolical tangents, $\tan(\beta_i h_i) \to j\tanh(\alpha_i h_i)$. The parameters α_i are the corresponding dissipation constants in the different media. However, the dispersion equations have real variables in all cases. For example, the dispersion equation of TM_{0m0} mode in resonance cavity R2 with a single layer should be

simply rewritten as

$$\left(\frac{\beta_1}{\varepsilon_1}\tan\beta_1 h_1 - \frac{\alpha_3}{\varepsilon_3}\tanh\alpha_3 h_3\right) = 0 \qquad (2')$$

(for comparison, $\alpha_3 = 0$ is the dispersion equation of this mode for an empty cavity).

FORTRAN-code based software MLAYER.EXE has been developed to solve the corresponding dispersion equations. Its first option is the determination of a full-mode spectrum in the cavity with a sample (simplifying the mode identification during the measurements). As a second option it allows the determination of the unknown constants $\varepsilon'_{||}$ and $\varepsilon'_{\perp}$ of single- or multi-layer samples, if the resonance frequency of a given mode is measured and the other layers have known dielectric constants (the last known as an extraction procedure). Finally, the software accomplishes an error analysis, if the measuring errors of the geometrical and resonance parameters have been determined preliminary.

2.2 Determination of the Dielectric Loss Tangent in Single-Layer Samples

The determination of the dielectric loss tangent (longitudinal and transversal values $\tan\delta_{\varepsilon||}$ and $\tan\delta_{\varepsilon\perp}$) of a single-layer sample is more complicated compared to the determination of the corresponding real part of the dielectric constants, $\varepsilon'_{||}$ and $\varepsilon'_{\perp}$.

Two different approaches could be used. In a direct approach the dielectric constants of all resonator parts are considered as complex parameters, $\varepsilon_i = \varepsilon'_i(1 - j\tan\delta_{\varepsilon i})$, and the resonator walls have to be described with a finite conductivity $\sigma_W <\propto$. These assumptions lead to complex dispersion equations, but now additional boundary conditions at the finite-conductivity walls should be taken into account (see [22], pp. 534–536). Extra parameters have to be measured: the complex resonance frequency $f_{res} = f_\varepsilon[1 + j(1/2Q_{0\varepsilon})]$ (f_ε is the real resonance frequency, $Q_{0\varepsilon}$ is the unloaded quality factor of the cavity with the sample) and the surface resistance R_s of the cavity walls. This direct method is suitable for characterization of very lossy samples (like absorbers, ferrites, semiconductors, *etc.* [23–25]), for which the energy dissipation leads to a noticeable shift of the resonance frequency in addition to a change of the quality factor. If the influence of this dissipation over the resonance frequency could be neglected, independent measurements of the dielectric constant and the dielectric loss tangent are possible for low- and medium-loss materials (like reinforced artificial substrates, sheets, thin films, *etc.*). This second approach is based on the representation of the cavity Q-factor in terms of integrals of the electric and magnetic fields squares [22] or in terms of the reactance-slope parameters [26] of the measurement resonance cavity with the sample. For this purpose, we could express the quality factor of the cavity using the stored energy and dissipated

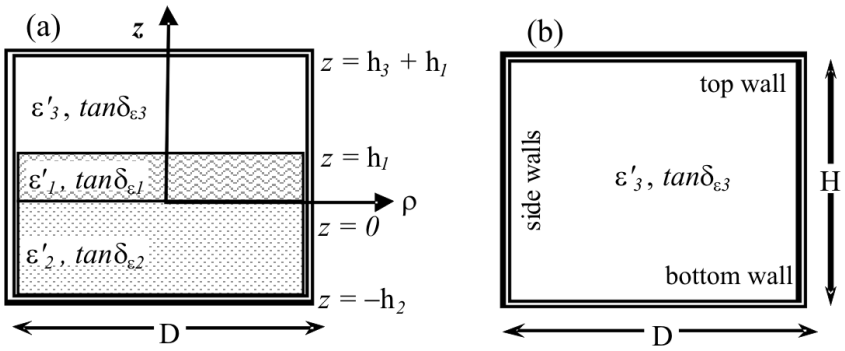

Figure 2. Generalized resonator ($D = D_{1,2}$; $H = H_{1,2}$), filled with lossy materials: (a) with single-layer sample with longitudinal or perpendicular parameters ε'_1, $\tan\delta_{\varepsilon 1}$; (b) without sample; empty (or foam-filled) cavity.

power in all three dielectric parts, which means an analytical calculation of 22 integrals for TE_{nmp} and TM_{0m0} modes.

Let us consider a single-layer sample as homogeneous, but anisotropic "averaged" layer with parameters ε'_1 and $\tan\delta_{\varepsilon 1}$ with height h_1 (see Figure 2). The pair of parameters represents either longitudinal values ($\varepsilon'_{1||}$, $\tan\delta_{\varepsilon 1||}$) in resonator R1 ($\mathrm{TE}_{0mp}$ modes) or transversal values ($\varepsilon'_{1\perp}$, $\tan\delta_{\varepsilon 1\perp}$) in resonator R2 ($\mathrm{TM}_{0m0}$ modes). It is assumed that the dielectric constant ε'_1 of this "averaged" layer is already determined by solving single-layer equations (1) (for $\varepsilon'_{1||}$) or (2) (for $\varepsilon'_{1\perp}$).

For determination of the unknown parameter $\tan\delta_{\varepsilon 1}$ we express the unloaded Q-factor of the resonators with sample as

$$Q_{0\varepsilon} = \omega \frac{W_1 + W_2 + W_3}{P_1 + P_2 + P_3 + P_{W1} + P_{W2} + P_{W3} + P_{\text{top}} + P_{\text{bottom}}}, \qquad (3)$$

where $W_{1,2,3}$ are the values of the stored energy in the considered three parts of the resonance cavity; $P_{1,2,3}$ are the dissipated powers within these parts due to the dielectric losses; P_{W1}, P_{W2}, P_{W3} are the powers, dissipated in the cavity side walls in corresponding regions; $P_{\text{top, bottom}}$ are the powers, dissipated in both cavity flanges; $\omega = \pi f_\varepsilon$. All these quantities are time-averaged. W_2, P_2, $P_{W2} = 0$ in the resonator R2. The unknown parameter $\tan\delta_{\varepsilon 1}$ occurs only in the expression for the dissipated power $P_1 = \tan\delta_{\varepsilon 1}\omega W_1$. Therefore, we get

$$\tan\delta_{\varepsilon 1} = P_1/\omega\, W_1, \qquad (4)$$

where

$$P_1 = \omega \frac{W_1 + W_2 + W_3}{Q_{0\varepsilon}} - (P_2 + P_3 + P_{W1} + P_{W2} + P_{W3} + P_{\text{top}} + P_{\text{bottom}})\,. \qquad (5)$$

We can separately express the energy and power terms in (5) for the resonators R1 and R2 similarly to the calculation procedure described in [27] (see also [4]). The stored-energy and dissipated-power terms are defined as

$$W_1 = \frac{\varepsilon_1' \varepsilon_0}{2} \int_{z=0}^{h_1} \int_{\varphi=0}^{2\pi} \int_{\rho=0}^{R} \left| E^{(1)} \right|^2 \rho \, d\rho \, d\varphi \, dz \tag{6.1}$$

$$W_2 = \frac{\varepsilon_2' \varepsilon_0}{2} \int_{z=-h_2}^{0} \int_{\varphi=0}^{2\pi} \int_{\rho=0}^{R} \left| E^{(2)} \right|^2 \rho \, d\rho \, d\varphi \, dz \tag{6.2}$$

$$W_3 = \frac{\varepsilon_3' \varepsilon_0}{2} \int_{z=h_1}^{h_1+h_3} \int_{\varphi=0}^{2\pi} \int_{\rho=0}^{R} \left| E^{(3)} \right|^2 \rho \, d\rho \, d\varphi \, dz \tag{6.3}$$

$$P_2 = \tan \delta_{\varepsilon 2} \omega W_2 \tag{7.1}$$

$$P_3 = \tan \delta_{\varepsilon 3} \omega W_3 \tag{7.2}$$

$$P_{W1} = \frac{R_s}{2} \int_{z=0}^{h_1} \int_{\varphi=0}^{2\pi} \left| H_t^{(1)} \right|^2 \rho \, d\varphi \, dz \mid_{\rho=R} \tag{8.1}$$

$$P_{W2} = \frac{R_s}{2} \int_{z=-h_2}^{0} \int_{\varphi=0}^{2\pi} \left| H_t^{(2)} \right|^2 \rho \, d\varphi \, dz \mid_{\rho=R} \tag{8.2}$$

$$P_{W3} = \frac{R_s}{2} \int_{z=h_1}^{h_1+h_3} \int_{\varphi=0}^{2\pi} \left| H_t^{(3)} \right|^2 \rho \, d\varphi \, dz \mid_{\rho=R} \tag{8.3}$$

$$P_{bottom} = \frac{R_s}{2} \int_{\rho=0}^{R} \int_{\varphi=0}^{2\pi} \left| H_t^{(2)} \right|^2 \rho \, d\rho \, d\varphi \mid_{z=-h_2} \tag{9.1}$$

$$P_{top} = \frac{R_s}{2} \int_{\rho=0}^{R} \int_{\varphi=0}^{2\pi} \left| H_t^{(3)} \right|^2 \rho \, d\rho \, d\varphi \mid_{z=h_1+h_3}, \tag{9.2}$$

where $|E^{(k)}|^2$ are the squares of the total electric field in the separate resonator volumes (superscript $^{(k)}$ denotes the regions with upper indices $^{(1)}$, $^{(2)}$ or $^{(3)}$ in Figure 2); $|H_t^{(k)}|^2$ are the squares of the tangential magnetic-field components to the resonator wall surfaces; R_s is the surface impedance on these walls.

1) Case – resonator R1, TE_{0mp} modes ($R = R_1$; $H = H_1$): The azimuthally-symmetrical modes have three field components only – E_φ, H_ρ and H_z, which spatial dependences in the corresponding areas are given below (the time factor $\exp(j\omega t)$ is not included):

$$H_z^{(1)} = J_0(\tau_{0m}\rho)\ [A_0 \sin\beta_1 z + B_0 \cos\beta_1 z] \tag{10.1}$$

$$H_\rho^{(1)} = \frac{\beta_1}{\tau_{0m}} J_0'(\tau_{0m}\rho)\ [A_0 \cos\beta_1 z - B_0 \sin\beta_1 z] \tag{10.2}$$

$$E_\varphi^{(1)} = j\frac{\omega\mu_0}{\tau_{0m}} J_0'(\tau_{0m}\rho)\ [A_0 \sin\beta_1 z + B_0 \cos\beta_1 z] \tag{10.3}$$

$$H_z^{(2)} = C_0 J_0(\tau_{0m}\rho)\ [\sin\beta_2 z + \tan\beta_2 h_2 . \cos\beta_2 z] \tag{11.1}$$

$$H_\rho^{(2)} = C_0 \frac{\beta_2}{\tau_{0m}} J_0'(\tau_{0m}\rho)\ [\cos\beta_2 z - \tan\beta_2 h_2 . \sin\beta_2 z] \tag{11.2}$$

$$E_\varphi^{(2)} = jC_0 \frac{\omega\mu_0}{\tau_{0m}} J_0'(\tau_{0m}\rho)\ [\sin\beta_2 z + \tan\beta_2 h_2 . \cos\beta_2 z] \tag{11.3}$$

$$H_z^{(3)} = D_0 J_0(\tau_{0m}\rho)\ [\sin\beta_3 z - \tan\beta_3 (h_3 + h_1) . \cos\beta_3 z] \tag{12.1}$$

$$H_\rho^{(3)} = D_0 \frac{\beta_3}{\tau_{0m}} J_0'(\tau_{0m}\rho)\ [\cos\beta_3 z + \tan\beta_3 (h_3 + h_1) . \sin\beta_3 z] \tag{12.2}$$

$$E_\varphi^{(3)} = jD_0 \frac{\omega\mu_0}{\tau_{0m}} J_0'(\tau_{0m}\rho)\ [\sin\beta_3 z - \tan\beta_3 (h_3 + h_1) . \cos\beta_3 z]\,, \tag{12.3}$$

where $\tau_{0m} = (\chi_{0m})_{TE}/R$. The unknown constants A_0, B_0 and C_0 are connected with the following relations due to the boundary conditions – continuity of the tangential electric and magnetic field components at the surfaces between the cavity parts

$$A_0 = \frac{\beta_2}{\beta_1} C_0; \quad B_0 = C_0 \tan\beta_2 h_2; \quad \text{and}$$

$$D_0 = \frac{\beta_1}{\beta_3} C_0 \frac{\cos\beta_3 (h_3 + h_1)}{\cos\beta_3 h_3} \left[\frac{\beta_3}{\beta_1} \cos\beta_1 h_1 - \tan\beta_2 h_2 . \sin\beta_1 h_1\right]. \tag{13}$$

Now we have to substitute the field dependences (10.1)–(12.3) into the expressions (6.1)–(9.2) taking into account that $|E^{(k)}|^2 = |E_\varphi^{(k)}|^2$ in all regions, while the corresponding tangential magnetic fields are: $H_t^{(k)} = H_z^{(k)}$ at the side walls of the resonator and $H_t^{(2,3)} = H_\rho^{(2,3)}$ at the top and bottom flanges. For the energy-stored and dissipated-power terms in (5) we obtain the expressions (14.1)–(17.2) with the superscript $^{TE_{0m}}$ given below. The known properties of the trigonometrical and first-kind Bessel functions and the equality

$J_0'(\tau_{0m}R) = 0$ for TE_{0mp} modes are used for the analytical calculations

$$W_1^{TE_{0m}} = V_1^{TE_{0m}} J_0^2(\tau_{0m}R)\ \left(A_0^2 X_1^{TE_{0m}} + B_0^2 Y_1^{TE_{0m}} + 2A_0B_0 Z_1^{TE_{0m}}\right) \tag{14.1}$$

$$P_{W1}^{TE_{0m}} = S_1^{TE_{0m}} J_0^2(\tau_{0m}R)\ \left(A_0^2 X_1^{TE_{0m}} + B_0^2 Y_1^{TE_{0m}} + 2A_0B_0 Z_1^{TE_{0m}}\right) \tag{14.2}$$

$$W_2^{TE_{0m}} = V_2^{TE_{0m}} J_0^2(\tau_{0m}R)\ C_0^2 X_2^{TE_{0m}} / \cos^2\beta_2 h_2 \tag{15.1}$$

$$P_{W2}^{TE_{0m}} = S_2^{TE_{0m}} J_0^2(\tau_{0m}R)\ C_0^2 X_2^{TE_{0m}} / \cos^2\beta_2 h_2 \tag{15.2}$$

$$W_3^{TE_{0m}} = V_3^{TE_{0m}} J_0^2(\tau_{0m}R)\ D_0^2 X_3^{TE_{0m}} / \cos^2\beta_3 (h_3 + h_1) \tag{16.1}$$

$$P_{W3}^{TE_{0m}} = S_3^{TE_{0m}} J_0^2(\tau_{0m}R)\ D_0^2 X_3^{TE_{0m}} / \cos^2\beta_3 (h_3 + h_1) \tag{16.2}$$

$$P_{bottom}^{TE_{0m}} = T_2^{TE_{0m}} J_0^2(\tau_{0m}R)\ C_0^2 / \cos^2\beta_2 h_2 \tag{17.1}$$

$$P_{top}^{TE_{0m}} = T_3^{TE_{0m}} J_0^2(\tau_{0m}R)\ D_0^2 / \cos^2\beta_3 (h_3 + h_1). \tag{17.2}$$

The following denotations are used above:

$$V_k^{TE_{0m}} = \varepsilon_k'(\omega/c)^2 \mu_0 \pi R^2 h_k / 4\tau_{0m}^2;\ k = 1,\ 2,\ 3) \tag{18.1}$$

$$S_k^{TE_{0m}} = R_s^{TE_{0m}} \pi R h_k / 2;\ (k = 1,\ 2,\ 3) \tag{18.2}$$

$$T_k^{TE_{0m}} = R_s^{TE_{0m}} \pi R^2 \beta_k^2 / 2\tau_{0m}^2;\ (k =\ 2,\ 3) \tag{18.3}$$

$$X_k^{TE_{0m}} = [\ 1 - \sin(2\beta_k h_k)/2\beta_k h_k]\,;\ (k = 1,\ 2,\ 3) \tag{19.1}$$

$$Y_1^{TE_{0m}} = [\ 1 + \sin(2\beta_1 h_1)/2\beta_1 h_1] \tag{19.2}$$

$$Z_1^{TE_{0m}} = [\ 1 - \cos(2\beta_1 h_1)]\,/2\beta_1 h_1. \tag{19.3}$$

Finally, we can calculate the necessary value of the longitudinal dielectric loss tangent $\tan\delta_{\varepsilon 1||}$ of the middle layer substituting the energy and power terms from (14.1)–(17.2) into (4, 5). The only unknown parameter is the surface resistance R_s, which could be determined from measurements of the empty resonator R1 (see Section 4) for details).

2) Case – resonator R2, TM_{0m0} modes (h_2= 0; $R = R_2$; $H = H_2$): These modes also have three field components E_ρ, E_z and H_φ; their spatial dependences are presented by the expressions (20.1)–(21.3):

$$E_z^{(1)} = E_0 J_0(\tau_{0m}\rho)\ \cos\beta_1 z \tag{20.1}$$

$$E_\rho^{(1)} = -E_0 \frac{\beta_1}{\tau_{0m}} J_0'(\tau_{0m}\rho)\ \sin\beta_1 z \tag{20.2}$$

$$H_\varphi^{(1)} = -jE_0 \frac{\omega\varepsilon_0\varepsilon_1'}{\tau_{0m}} J_0'(\tau_{0m}\rho)\cos(\beta_1 z) \tag{20.3}$$

$$E_z^{(3)} = F_0 J_0(\tau_{0m}\rho)\ [\tan\beta_3(h_3+h_1).\sin\beta_3 z + \cos\beta_3 z] \tag{21.1}$$

$$E_\rho^{(3)} = F_0 \frac{\beta_3}{\tau_{0m}} J_0'(\tau_{0m}\rho)\ [\tan\beta_3(h_3+h_1).\cos\beta_3 z - \sin\beta_3 z] \tag{21.2}$$

$$H_\varphi^{(3)} = -jF_0 \frac{\omega\varepsilon_0\varepsilon_3'}{\tau_{0m}} J_0'(\tau_{0m}\rho)\ [\tan\beta_3(h_3+h_1).\sin\beta_3 z + \cos\beta_3 z]\,, \tag{21.3}$$

where $\theta_{0m} = (\chi_{0m})_{TM}/R$. The unknown constants in this case are only two, E_0 and F_0 and the relation between them is

$$F_0 = E_0 \frac{\varepsilon_1'}{\varepsilon_3'}.\frac{\cos\beta_1 h_1.\cos\beta_3 H}{\cos\beta_3 h_3}. \tag{22}$$

In this case we can use other expressions for the energy and power terms (with superscript $^{TM_{0m}}$) in (5). The square of the total electric field now is $|E^{(k)}|^2 = |E_\rho^{(k)}|^2 + |E_z^{(k)}|^2$, while the tangential magnetic field is $H_t^{(k)} = H_\varphi^{(k)}$ everywhere. The equality $J_0(\theta_{0m}R) = 0$ for the TM_{0m0} modes is valid. After new substitutions of the field dependences from (20.1)–(21.3) into (6.1)–(9.2) ($h_2 = 0$; $H_2 = h_3 + h_1$), we get

$$W_1^{TM_{0m}} = V_1^{TM_{0m}} J_1^2(\theta_{0m}R)\, E_0^2 \left(X_1^{TM_{0m}} + Y_1^{TM_{0m}}\right) \tag{23.1}$$

$$P_{W1}^{TM_{0m}} = S_1^{TE_{0m}} J_1^2(\theta_{0m}R)\, E_0^2\, Y_1^{TM_{0m}} \tag{23.2}$$

$$W_3^{TM_{0m}} = V_3^{TM_{0m}} J_1^2(\theta_{0m}R) F_0^2 \left(X_1^{TM_{0m}} + Y_1^{TM_{0m}}\right) / \cos^2\beta_3 H \tag{24.1}$$

$$P_{W3}^{TM_{0m}} = S_3^{TM_{0m}} J_1^2(\theta_{0m}R)\ F_0^2 Y_3^{TM_{0m}} / \cos^2\beta_3 H \tag{24.2}$$

$$P_{bottom}^{TM_{0m}} = T_\Sigma^{TM_{0m}} J_1^2(\theta_{0m}R)\ E_0^2 \tag{25.1}$$

$$P_{top}^{TM_{0m}} = T_3^{TM_{0m}} J_1^2(\theta_{0m}R)\ F_0^2 / \cos^2\beta_3 H, \tag{25.2}$$

where:

$$V_k^{TM_{0m}} = \varepsilon_k'\varepsilon_0\pi R^2 h_k/4\ (k = 1,\ \ 3) \tag{26.1}$$

$$S_k^{TM_{0m}} = R_s^{TM_{0m}} \varepsilon'^2_k \varepsilon_0 (\omega/c)^2 \pi R h_k / 2\mu_0\tau_{0m}^2 \tag{26.2}$$

$$T_k^{TM_{0m}} = R_S \varepsilon'^2_k \varepsilon_0 (\omega/c)^2 \pi R^2 / 2\mu_0\tau_{0m}^2 \tag{26.3}$$

$$X_k^{TM_{0m}} = \left(\beta_k^2/\tau_{0m}^2\right)\ [\,1 - \sin(2\beta_k h_k)/2\beta_k h_k] \tag{27.1}$$

$$Y_k^{TM_{0m}} = [\,1 + \sin(2\beta_k h_k)/2\beta_k h_k]\,. \tag{27.2}$$

The value of the transversal dielectric loss tangent $\tan\delta_{\varepsilon 1\perp}$ of the single layer sample could be computed from (4, 5) by the substitution of the energy and

power terms from (23.1)–(25.2). In this case the unknown surface resistance R_s is also determined from the measurement results of the empty resonator R2.

3) Determination of the surface resistance: There are two possibilities to obtain the value of the surface resistance. The simplest way is to use the known formula [28, pp. 25–26]

$$R_s = \sqrt{\pi f_\varepsilon \mu_W \mu_0 / \sigma_W}, \tag{28}$$

where σ_W is the catalogue value of the wall conductivity and μ_W is the relative wall permeability.

A more accurate way is the preliminary determination of the actual value of the surface resistance as in [29,30] for the measurement of the dielectric rod samples, or as in [31] for the characterization of HTS films. In our case we use the measurement results, namely the resonance frequency $\omega_e = 2\pi f_e$ and the unloaded Q-factor Q_{0e} of the empty (or foam-filled) resonators in order to calculate the actual value of R_s in each resonator (one average value for all resonator walls)

$$R_{s,e}^{TE_{0m}} = \frac{\varepsilon_3'(\omega_e/c)^2 \omega_e \mu_0 H_1}{4\tau_{0m}^2} \left(\frac{1}{Q_{0e}^{TE_{0m}}} - \tan\delta_{\varepsilon 3}\right) \left(\frac{H_1}{2R_1} + \frac{\beta_3^2}{\tau_{0m}^2}\right)^{-1} \tag{29}$$

for the resonator R1 and

$$R_{s,e}^{TM_{0m}} = \frac{H\theta_{0m}^2}{2\omega_e \varepsilon_3' \varepsilon_0 (1 + H_2/R_2)} \left(\frac{1}{Q_{0e}^{TM_{0m}}} - \tan\delta_{\varepsilon 3}\right) \tag{30}$$

for the resonator R2. Using the computed values for R_s (at the frequency f_e) we can get a pair of equivalent values σ_{Weq} of the wall conductivity for each measurement resonator from

$$\sigma_{Weq} = \pi f_e \mu_W \mu_0 / R_s^2. \tag{31}$$

Both equivalent values of σ_{Weq} should be used in (28) in order to recalculate the surface resistances $(R_s)_{TE,TM}$ at the resonance frequency f_ε of the cavities with the sample. Then, the expressions (18.2–3) and (26.2–3) with the actual values σ_{Weq} can be used for the calculation of the dielectric loss tangent in each direction.

3 Measurement Sensitivity and Errors

3.1 Measuring Resonance Cavities

There are two possibilities to realize the proposed two-resonator method. 1) Both measuring resonators have equal diameters $D_1 = D_2$ and the measurement of $\varepsilon_{||}'$ and $\varepsilon_{\perp}'$ corresponds to two different resonance frequencies denoted as $f_\varepsilon^{TE011} > f_\varepsilon^{TM010}$ or 2) The resonators have diameters $D_1 > D_2$,

for which the values of $\varepsilon'_{||}$ and $\varepsilon'_{\perp}$ are determined at relatively close frequencies $f_{\varepsilon}^{TE011} \sim f_{\varepsilon}^{TM010}$. One non-metallized sample is needed for the first case, while two separate samples with different diameters have to be prepared for the second case. In this paper we present examples for the first case only, because it is more suitable for materials with a relatively weak frequency dependence of the dielectric constant and loss tangent. Moreover, the variations in the parameters from sample to sample could be avoided. The resonator dimensions are designed to be $D_1 = 30.00$ mm, $H_1 = 29.82$ mm (for R1); $D_2 = 30.00$ mm, $H_2 = 12.12$ mm (for R2). The corresponding measured resonance frequencies and unloaded Q-factors of the empty resonators are $f_e^{TE011} = 13.1519$ GHz, $Q_{0e}^{TE011} = 14470$ for R1 and $f_e^{TM010} = 7.6385$ GHz, $Q_{0e}^{TM010} = 3850$ for R2. All these parameters are obtained with "daily" variations of $\pm 0.01\%$ for the resonance frequency and $\pm 1.5\%$ for the Q-factor (mainly due to room temperature changes, cavity cleanness and influence of the tuning elements).

Thus, the values $\varepsilon'_{||}$, $\tan\delta_{\varepsilon||}$ could be measured in the frequency range ~9–13.15 GHz (TE_{011} mode), while the values $\varepsilon'_{\perp}$, $\tan\delta_{\varepsilon\perp}$ – in the range ~5.5–7.63 GHz (TM_{010} mode) – Figure 3.

The measuring resonators R1 and R2 are designed to have special features concerning the working conditions; nevertheless they are cylindrical resonance cavities (see [4] for details). Resonator R1 has two movable "contact-less" flanges with absorbing rings in order to suppress the unwanted here TM modes (compression better than – 60 dB). Two SMA connectors at an azimuthal angle of

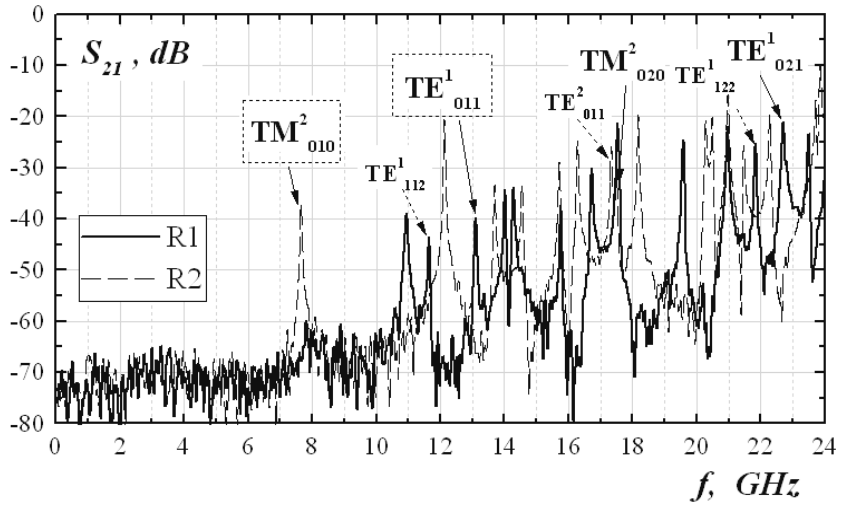

Figure 3. Frequency responses of the R1 and R2 resonators in a transmitted-power regime. The resonance curves of the discussed modes are marked.

90° slightly below the middle of the resonator with exciting semi loops with axis parallel to the resonator axis are arranged on the cavity side walls. Thus, the excited symmetrical TE_{011}, TE_{021}, TE_{013}, ... modes are suitable at these conditions for measurement purposes of the longitudinal dielectric parameters, while the TE_{012}, TE_{014}, ... modes are not. A limitation is observed with the excitations of parasitic TE_{112}, TE_{122}, ... modes, which are not sensitive to the dielectric sample placed in the resonator's half-height. For example, coincidence between the resonance curves of the TE_{011} and TE_{112} modes restricts the dielectric parameters' measurement at this frequency. Another problem is the sample positioning in R1. Two thin screw holders are used to press the sample laterally, but a pair of low-loss foam supports is also applicable.

Resonator R2 has one movable flange with an improved DC contact and two SMA connectors at 180° in the resonator middle with exciting semi-loops axis perpendicularly to the resonator axis. Only a resonator height reduction ($H_2 < R_2$) is used here to ensure the single-mode regime below 12 GHz for measurements of the transversal dielectric parameters using the lowest-order TM_{010} mode. Measurements with TM_{020}, TM_{030} modes are also possible, but the near presence of parasitic high-order modes makes the mode identification more difficult.

3.2 Measurement Errors

We present in this Section a short analysis of the measuring errors. The main sources of errors in the proposed two-resonator method are due to the uncertainties in the determination of the parameters D, H, h_i, f_ε and the sample positioning in the resonance cavities. Measurements of the resonance frequencies are usually precise; therefore, the measuring errors mainly depend on the geometrical parameters. However, a detectable difference is usually observed between the measured $(f_e)_{meas}$ and calculated $(f_e)_{calc}$ resonance frequencies in both empty resonators due to a variety of reasons: coupling effects of connectors, influence of supporting screws, resonator elliptical eccentricity, contact-less flange influence in R1, holes influence in R2, *etc.* A suitable solution of this problem is to introduce an *equivalent cavity diameter* $(D_{eq})_{\text{TE, TM}}$ for each of the considered modes in order to ensure the exact equality $(f_e)_{meas\,\text{TE,TM}} \equiv (f_e)_{calc\,\text{TE,TM}}$ (± 0.1 – % deviation) in both of the empty resonators. We obtained the following equivalent diameters: $(D_{eq})_{\text{TE011}} = 30.086$ mm (0.29% increase) and $(D_{eq})_{\text{TM010}} = 30.045$ mm (0.15% increase). Thus, the use of D_{eq} instead of D allows a minimization of the uncertainties due to the resonator dimensions D and H. Therefore, the errors of the measurement of $\varepsilon'_{||}$ and $\varepsilon_\perp$ values mainly depend on the relative errors of the sample height determination $\Delta h_1/h_1$ and the sample positioning $\Delta h_3/h_3$ [4].

A similar problem appears for the unloaded Q-factors of the empty resonators; namely the measured value is smaller than the theoretical one. For exam-

ple, the theoretical Q-factor for the TE_{011} mode in R1 is $Q_{0e,th} = 22125$ for gold conductivity $\sigma_{\mathrm{Au}} = 4.1 \times 10^7$ S/m and theoretical surface resistance $R_{s,th} = 35.3$ mΩ (at $f_e = 13.1519$ GHz). The measured value is $Q_{0e} = 14470$, which corresponds to a measured surface resistance $R_{s,e} = 53.9$ mΩ, obtained from (29) and *equivalent conductivity* $\sigma_{Weq} = 1.8 \times 10^7$ S/m calculated from (31). The corresponding theoretical values for the TM_{010} mode in R2 are: $Q_{0e,th} = 7482$ and $R_{s,th} = 27.0$ mΩ (at $f_0 = 7.6385$ GHz), while the measured values are: $Q_{0e} = 3850$, $R_{s,e} = 52.5$ mΩ, obtained by (30) and an *equivalent conductivity* $\sigma_{Weq} = 1.1 \times 10^7$ S/m. These results unambiguously show that the determination of the equivalent wall conductivity for each working mode is absolutely necessary for a decrease in the relative errors of measurements of the loss tangent.

Thus, the equivalent parameters for the corresponding gold-plated cavities (R1 with TE_{011} mode and R2 with TM_{010} mode) could be calculated by the following closed-form expressions:

$$R_{eq1} = 182.824 H_1 \left(f_{e1}^2 H_1^2 - 22468.9\right)^{1/2} \tag{32.1}$$

$$R_{eq2} = 114.74274 / f_{e2} \tag{32.2}$$

$$\sigma_{eq1,2} = 3947.842 f_{e1,2} / R_{s1,2}^2, \tag{33}$$

where the surface resistance $R_{s1,2}$ (one average value for all walls of the resonator) is expressed as:

$$R_{s1} = 1.8798 \times 10^{-5} H_1 R_{eq1}^2 f_{e1}^3 \frac{1}{Q_{0e1}} \left[0.5 \frac{H_1}{R_{eq1}} - 1 + 2.9918 \times 10^{-5} (R_{eq1} f_{e1})^2 \right]^{-1} \tag{32}$$

$$R_{s2} = 0.5 H_2 \left(\frac{2.40483}{R_{eq2}} \right)^2 \frac{1}{Q_{0e2}} \left[5.56313 \times 10^{-5} f_{e2} \left(1 + \frac{H_2}{R_{eq2}} \right) \right]^{-1}. \tag{33}$$

All the geometrical dimensions $R_{eq1,2}$ and $H_{1,2}$ in the expressions (1)–(4) are in mm, $f_{e1,2}$ – in GHz, $R_{s1,2}$ – in Ohms and $\sigma_{eq1,2}$ – in S/m.

Taking into account the above-discussed issues the measuring errors in the presented method can be estimated as follows: < 1.0–1.5% for $\varepsilon'_{||}$ and $< 5\%$ for $\varepsilon'_{\perp}$ for a reference sample like RO3203 with a thickness of 0.254 mm measured with errors $\Delta h_1 / h_1 < 2\%$. Besides, even the positioning uncertainty $\Delta h_3 / h_3$ reaches a value of 10% (*i.e.* even $\Delta h_3 \sim \pm 1.5$ mm) for the sample positioning in R1, the relative measurement error of $\varepsilon'_{||}$ does not exceed the value of 2.5%. The measuring errors for the determination of the dielectric loss tangent are estimated as: 5–7% for $\tan \delta_{\varepsilon||}$, but up to 25% for $\tan \delta_{\varepsilon\perp}$, when the measuring error for the unloaded Q-factor is 5%.

3.3 Measurement Sensitivity

A real problem of the proposed method for determination of dielectric anisotropy ΔA_ε is the measurement sensitivity of the TM_{010} mode in the resonator R2 (for $\varepsilon_\perp$), which is noticeably smaller compared to the sensitivity of the TE_{011} mode in R1 (for $\varepsilon'_{||}$). The curves of the resonance frequency shift versus the dielectric constant (Figure 4) clearly illustrate this effect for one-layer samples with h_1 from 0.125 to 1.5 mm. The shift $\Delta f/\Delta\varepsilon$ in R1 for a sample with $h_1 = 0.5$ mm is a decrease of 480 MHz for doubling of $\varepsilon'_{||}$ (from 2 to 4), while the corresponding shift in R2 is only a decrease of 42.9 MHz only for doubling of $\varepsilon_\perp$. Also, the Q-factor of the TM_{010} mode in R2 is smaller compared to the Q-factor of the TE_{011} mode in R1. This leads to an unequal accuracy in the determination of the loss tangent anisotropy $\Delta A_{\tan\delta\varepsilon}$.

Thus, the measured anisotropy for the dielectric constant $\Delta A_\varepsilon < 2.5$-$3\%$ and for the dielectric loss tangent $\Delta A_{\tan\delta\varepsilon} < 10$–$12\%$ could be associated with a *practical isotropy* of the sample ($\varepsilon'_{||} \cong \varepsilon'_\perp$; $\tan\delta_{\varepsilon||} \cong \tan\delta_{\varepsilon\perp}$), because these differences fall into the measurement error margins.

We checked this assumption first for the well-known isotropic PTFE (Teflon) substrate – see data in Table 1 and Table 2 (averaged from at least 5 samples). We use TE_{011} and TE_{021} modes in the resonator R1 and TM_{010} and TM_{020} modes in the resonator R2, for which we determine the equivalent diameters $(D_{eq})_{\text{TE, TM}}$ and the equivalent wall conductivity $(\sigma_{Weq})_{\text{TE, TM}}$. The measured "anisotropy" ΔA_ε for the 1.03-mm thick PTFE sample is between values 0.25–1.2% for different combinations of data – *i.e.* the practical isotropy of the dielectric constant is confirmed. Very important is the fact, that if the physical diameters D_1 or D_2 are used in the calculation from the equations (1, 2), higher values will be

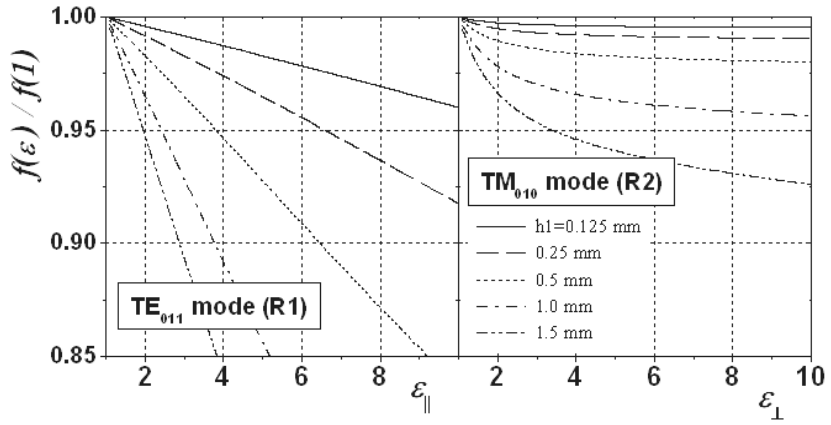

Figure 4. Measurement sensitivity of dielectric constant in cavities R1 and R2.

Table 1. Measured Dielectric Constant of PTFE Samples.

D_{eq} or D, mm	$\varepsilon_{\|\|}$ (in R1)	Mode f, GHz	D_{eq} or D, mm	$\varepsilon_{\perp}$ (in R2)	Mode f, GHz
30.086	2.045	TE_{011}	30.045	2.036	TM_{010}
30.00	2.105	12.6567	30.00	2.168	7.4624
30.081	2.044	TE_{021}	30.071	2.023	TM_{020}
30.00	2.092	21.7732	30.00	2.147	17.0158

Table 2. Measured Dielectric Loss Tangent of PTFE Samples.

σ_{eq} or σ, S/m	$\tan\delta_{\varepsilon\|\|}$ (in R1)	Mode $Q_{0\varepsilon}$	σ_{eq} or σ, S/m	$\tan\delta_{\varepsilon\perp}$ (in R2)	Mode $Q_{0\varepsilon}$
1.8×10^{7}	2.85×10^{-4}	TE_{011}	1.1×10^{7}	2.59×10^{-4}	TM_{010}
4.1×10^{7}	4.12×10^{-4}	9535	4.1×10^{7}	2.94×10^{-3}	3589
0.7×10^{7}	2.71×10^{-4}	TE_{021}	0.7×10^{7}	2.77×10^{-4}	TM_{020}
4.1×10^{7}	5.25×10^{-4}	7624	4.1×10^{7}	1.44×10^{-3}	4690

obtained compared to the known value 2.04–2.05 [32]. (For example, 3% for $\varepsilon'_{||}$ and 6.2% for $\varepsilon'_{\perp}$, while the measuring errors are only 0.6% for $\varepsilon'_{||}$ and 1.1% for $\varepsilon'_{\perp}$ in this case). The measured anisotropy $\Delta A_{\tan\delta\varepsilon}$ is higher, between 2.2–9.5% for different realized combinations, while the measuring uncertainties are smaller: $\sim$2.3% for $\tan\delta_{\varepsilon||}$ and $\sim$ 3.6% for $\tan\delta_{\varepsilon\perp}$. Another important conclusion is that the utilization of the equivalent conductivity σ_{Weq} has a decisive influence to the measurement accuracy for the determination of the dielectric loss tangent values in all cases. Actually, if we use $\sigma_{\mathrm{Au}} = 4.1 \times 10^{7}$ S/m (instead σ_{Weq}), we will obtain higher values for the dielectric loss tangent, from 1.4 up to 5.0 times higher (*e.g.* for $\tan\delta_{\varepsilon\perp}$, TM_{020} mode).

These preliminary investigations allow us to conclude that the proposed two-resonator method has the ability to detect the *practical isotropy* and, therefore, the *possible anisotropy* even for low-permittivity and low-loss materials as PTFE.

4 Measurement of the Dielectric Anisotropy of Single-Layer Substrates

This chapter includes data for the measured dielectric anisotropy of several commercial reinforced substrates. These artificial materials contain different numbers of built-in layers (depending on h_1) of woven glass with an appropriate filling and therefore, they may have more or less noticeable anisotropy. The catalogue data from the manufacturers do not include information about the actual values of ΔA_{ε} and $\Delta A_{\tan\delta\varepsilon}$.

Table 3. Measured Anisotropy ΔA_ε and $\Delta A_{\tan\delta\varepsilon}$ in Reinforced Substrates.

Substrate (h_1, mm)	$\varepsilon'_{\|\|}$	$\varepsilon'_\perp$	$\tan\delta_{\varepsilon\|\|}$	$\tan\delta_{\varepsilon\perp}$	IPC TM-650 2.5.5.5 @ 10 GHz
	ΔA_ε, %		$\Delta A_{\tan\delta\varepsilon}$, %		
RT/duriod 6002 (0.25)	2.92	2.89	0.00142	0.00135	2.94 / 0.0012
	1.0 ± 1		5 ± 3		
RO3003 (0.25)	3.02	2.93	0.0013	0.0013	3.00 / 0.0013
	3.0 ± 1		0 + 3		
RO3203 (0.25)	3.19	2.96	0.0026	0.0021	3.02 / 0.0016
	5.7 ± 2		21 ± 4		
RO4003 (0.21)	3.60	3.36	0.0032	0.0029	3.38 / 0.0027
	7.0 ± 2		11 ± 2		
Arlon CLTE (0.25)	3.10	2.78	0.0033	0.0023	2.98 / 0.0025
	11 ± 2		36 ± 5		
Taconic RF-35 (0.25)	3.78	3.22	0.0048	0.0032	3.50 / 0.0033
	16 ± 3		40 ± 6		
GETEK (R54) (0.25)	3.76	3.17	0.0045	0.0029	3.90 / 0.0046
	17 ± 3		43 ± 6		split post cavity
NH9300 (0.25)	3.49	2.80	0.0039	0.0023	3.00 / 0.0023
	22 ± 4		52 ± 7		
FR-4 (0.19)	4.45	3.73	0.0169	0.0184	4.7 / 0.020
	18 ± 3		9 ± 2		
RO3010 (0.25)	11.76	9.26	0.0024	0.0041	10.2 / 0.0035
	24 ± 4		52 ± 7		

We have measured and compared the anisotropy of a lot of modern RF substrates, but we present here data for some of them (see Table 3 for substrates with a relatively small thickness in the interval 0.2–0.3 mm). The measurement errors are estimated as 1.1–1.5% for dielectric constants and 8–15% for loss tangents all at 12.8 GHz for longitudinal values and at 7.6 GHz for transversal ones. According to the measured anisotropy the artificial substrates could be classified as: 1) near-to-isotropic substrates, $\Delta A_\varepsilon < 2$–5%, $\Delta A_{\tan\delta\varepsilon} < 10\%$ (RT/ Duroid 6002, Rogers RO3003); 2) substrates with relatively small anisotropy $\Delta A_\varepsilon \sim 5$–$15\%$, $\Delta A_{\tan\delta\varepsilon} \sim 10$–$30\%$ (RO4003, RO3203, Arlon CLTE); 3) substrates with noticeable and big anisotropy, $\Delta A_\varepsilon > 15\%$, $\Delta A_{\tan\delta\varepsilon} > 30\%$ (Neltec NH9300, Taconic RF-35, GETEK, RO3010). It is a big problem for the RF designers that most of the catalogue data includes just one value for $\varepsilon_\perp$ of the substrate sheets for all standard thicknesses. The method proposed in this paper allows to obtain a dependence of the dielectric anisotropy versus the substrate thickness in a wide frequency range (see data in Table 4 for the popular RO4003 laminate). Our results show that the average dielectric-constant anisotropy of this material does not practically change, $\Delta A_\varepsilon \sim 6.5$–$8\%$, while the loss-tangent anisotropy $\Delta A_{\tan\delta\varepsilon}$ increases from 11% up to 51% for substrates with a thick-

Table 4. Measured Dielectric Parameters of RO4003 Substrates with Different Thickness.

h_1, mm (actual value)	$\varepsilon'_{\|\|}/f_\varepsilon$, GHz (1st row) $\tan\delta_{\varepsilon\|\|}/Q_{0\varepsilon}$ (2nd row)		$\varepsilon'_{\perp}/f_\varepsilon$, GHz (1st row) $\tan\delta_{\varepsilon\perp}/Q_{0\varepsilon}$ (2nd row)	
	TE_{011}	TE_{021}	TM_{010}	TM_{020}
0.205	3.603/12.9096 3.24×10^{-3}/4305	3.617/22.3406 3.23×10^{-3}/3376	3.361/7.5922 2.94×10^{-3}/3614	3.405/17.4036 3.14×10^{-3}/5075
0.52	3.610/12.5150 3.20×10^{-3}/1889	3.623/21.4019 3.78×10^{-3}/1120	3.357/7.5179 2.61×10^{-3}/3305	3.391/17.1863 3.15×10^{-3}/3953
0.82	3.656/12.1188 4.06×10^{-3}/1043	3.640/20.3891 4.80×10^{-3}/635	3.370/7.4425 2.63×10^{-3}/3019	3.36/16.9207 2.86×10^{-3}/2901
1.53	3.591/11.3111 3.59×10^{-3}/754	3.594/18.4497 4.67×10^{-3}/461	3.350/7.2496 2.39×10^{-3}/2478	3.355/15.9967 2.52×10^{-3}/1339
catalogue data: $\varepsilon'_{\perp}=3.38$; $\tan\delta_{\varepsilon\perp}=2.0\times10^{-3}$ (10 GHz) (IPC TM-650 2.5.5.5)				

Table 4 (continue). Averaged Anisotropy in RO4003 Substrates with Different Thickness in the Frequency Range 7–22 GHz.

h_1, mm	$\varepsilon'_{\|\|}$	$\varepsilon'_{\perp}$	ΔA_ε, %	$\tan\delta_{\varepsilon\|\|}$	$\tan\delta_{\varepsilon\perp}$	$\Delta A_{\tan\delta\varepsilon}$, %
0.205	3.610	3.383	6.5	3.24×10^{-3}	2.90×10^{-3}	11
0.520	3.617	3.374	7.0	3.39×10^{-3}	2.88×10^{-3}	16
0.820	3.648	3.365	8.1	4.43×10^{-3}	2.75×10^{-3}	47
1.530	3.593	3.353	6.9	4.13×10^{-3}	2.46×10^{-3}	51

ness of 0.2–1.53 mm probably due to built-in air-gap inhomogeneities into the thicker substrates. Finally, the considered method allows an easy estimation of the statistical variations and standard deviations of the dielectric parameters for many samples (more than 50) extracted from different parts of large-size panels delivered from manufacturers [6].

5 Conclusions

We develop in this paper a relatively simple two-resonator method for determination of the anisotropy ΔA_ε of the dielectric constant and the anisotropy $\Delta A_{\tan\delta\varepsilon}$ of the dielectric loss tangent in small disk-shaped single-layer samples. The measuring errors are evaluated as small enough: $< 1.5\%$ for $\varepsilon'_{||}$, $< 5\%$ for $\varepsilon_\perp$, $< 5\%$ for $\tan\delta_{\varepsilon||}$ and $< 15\%$ for $\tan\delta_{\varepsilon\perp}$ in the case of typical substrates like RO3203 (0.254-mm thick). The relatively good accuracy is achieved mainly due to the use of the introduced equivalent parameters – equivalent resonator diameter and equivalent wall conductivity with their "daily" variations. Therefore, one can conclude that the described method has the ability to detect a possible anisotropy of single-layer materials for many practical cases. The presented examples fully confirm the efficiency of the proposed method to

easily test the dielectric anisotropy of the commercial reinforced substrates. The described method is not considered as a reference method for an accurate characterization of materials in special laboratories. Contrariwise, it is proposed for a realization by the users under working conditions. Therefore, the two-resonator method could be helpful in the RF designer's practice for an easy collection of accurate enough dielectric parameters of materials to be used in modern simulators to realize more accurate simulations than currently possible in an isotropic approximation.

Acknowledgment

The authors thank to the Scientific Research Found of University of Sofia "St. Kliment Ohridski" for the partial support.

References

[1] IPC TM-650 2.5.5.5 (1998) *Test Methods Manual*, `http://www.ipc.org/html/fsstandards.htm`.

[2] S.A. Ivanov and P.I. Dankov (2002) *J. Electrical Engineering (Slovakia)* Vol. **53** No. 9s pp. 93–95.

[3] P.I. Dankov and S.A. Ivanov (2004) *in Proc. 34th European Microwave Conf.*, Amsterdam, Holand, pp. 753–756.

[4] P.I. Dankov (2006) *IEEE Trans. Microwave Theory Tech.*, MTT-54, pp. 1534–1544.

[5] E. Drake, R.R. Boix, M. Horno, T.K. Sarkar (2000) *IEEE Trans. Microwave Theory Tech.*, MTT-48, pp. 1394–1403.

[6] P. Dankov, S. Kamenopolsky, and V. Boyanov (2003) in *Proc. 14th Microcoll' 2003*, Budapest, Hungary, pp. 217–220.

[7] P. Dankov (2004) in *Proc. 15th Int. Conf. on Microwave, Radar and Wireless Comm. MIKON'2004*, Warsaw, Poland, pp. 217–220.

[8] J. Baker-Jarvis, R.G. Geyer, J.H. Grosvenor, M.D. Janezic, C.A. Jones, B. Riddle, C.M. Weil and J. Krupka (1998) *IEEE Trans. Dielect. Elect. Insulation*, DEI-5, No. 4, pp. 571–577.

[9] Electromagnetic Properties of Materials, Radio-Frequency Technology Division, Electronic and Electrical Engineering Laboratory, NIST, USA, `http://www.boulder.nist.gov/div813/emagprop.htm`.

[10] RF and Microwave Dielectric and Magnetic Measurements, Electro-magnetic Material Characterization, EMMA-Club, National Physics Laboratory, UK, `http://www.npl.co.uk/electromagnetic/rfmffnewcal/rfmwdielectrics.html`.

[11] W.E. Courtney (1970) *IEEE Trans. Microwave Theory Tech.*, MTT-18, pp. 476–485.

[12] G. Kent (1988) *IEEE Trans. Microwave Theory Tech.*, MTT-36, pp. 1451–1454.

[13] E. Vanzura, R. Geyer, and M. Janezic (1993) NIST, Tech. Note 1354.

[14] M.D. Janezic and J. Baker-Jarvis (1999) *IEEE Trans. Microwave Theory Tech.*, MTT-47, pp. 2014–2020.

[15] X. Zhao, C. Liu and L. C. Shen, *IEEE Trans. Microwave Theory Tech.*, MTT-40, pp. 1951-1958, Oct. 1992

[16] J. Baker-Jarvis, B. F. Riddle (1996) NIST, Tech. Note 1384.

[17] J. Krupka, D. Cros, M. Aubourg, P. Giullion (1994) *IEEE Trans. Microwave Theory Tech.*, MTT-42, pp. 56–61.

[18] J. Krupka, K. Derzakowski, A. Abramowicz, M. Tobar and R.G. Gayer (1997) *IEEE MTT-S Int. Microwave Symp. Digest*, pp. 1347–1350.

[19] M. Olyphant, Jr. (1979) *IEEE MTT-S Int. Microwave Symp. Digest* pp. 91–93.

[20] G. Momcu, K. Sertel, J.L. Volakis (2008) *IEEE Trans. Microwave Theory Tech.*, MTT-56, pp. 217–223.

[21] R. F. Harrington (1961), *Time-Harmonic Electromagnetic Field*, New York, McGrow-Hill Book Company Inc., Chapter 5.

[22] R.E. Collin (1992) *Foundation for Microwave Engineering*, Second Edition, New York, McGrow-Hill Inc., Chapter 7.

[23] Y. Kobayashi and S. Tanaka (1980) *IEEE Trans. Microwave Theory Tech.*, MTT-28, pp. 1077–1085.

[24] C. Shieblich (1989) *IEEE Trans. Microwave Theory Tech.*, MTT-37, pp. 1555–1561.

[25] P.I. Dankov and S.T. Ivanov (1994) in *Proc. 12th Int. Conf. on Microwave Ferrites*, Bulgaria, pp. 27–32

[26] B.E. Spielman (2004) *IEEE Trans. Microwave Theory Tech.*, MTT-52, pp. 1683–1692.

[27] M.D. Janezic, E.F. Kuester, J. Baker-Jarvis (2003) in *Proc. 2003 IMAPS Ceramic Interconnect Technology Conf*, Denver, `http://www.boulder.nist.gov/div813/rfelec/properties/Pages/publications.html`.

[28] B.C. Wadell (1991) *Transmission-Line Design Handbook*, Boston, London, Artech House Inc., Chapter 2.

[29] Y. Kobayashi and M. Katoh (1985) *IEEE Trans. Microwave Theory Tech.*, MTT-33, pp. 586–592.

[30] A.P. Mourachkine and A.R.F. Barel (1995) *IEEE Trans. Microwave Theory Tech.*, MTT-43, pp. 544–551.

[31] Y. Kobayashi and H. Yoshikawa (1998) *IEEE Trans. Microwave Theory Tech.*, MTT-46, pp. 2524–2530.

[32] W.R. Humbert, W.R. Scott (1996) *IEEE Microwave and Guided Wave Lett.* vol. **6** pp. 262–264.